

# The Welded Heat-Affected Zone in Nickel Base Alloy 718

Control of the weld shape and grain size by proper attention to welding parameters improves weld soundness

BY M. J. LUCAS, JR., AND C. E. JACKSON

**ABSTRACT.** Nickel-base alloy 718 is a precipitation-hardening alloy used for high temperature applications. This alloy is one of the most readily weldable of the precipitation hardened nickel-base alloys. However, when the electron beam process is used, microcracking may occur in the heat-affected zone. These cracks can be very harmful in fatigue applications. It is this microcracking problem which prompted this investigation.

The objective of this investigation on nickel-base alloy 718 was to determine what changes occur in the heat-affected zone during welding. Bead-on-plate welds were made with the gas tungsten-arc and electron beam processes. The heat-affected zone was studied with reference to hardness, phases present, grain size and microcracking tendency.

Bead-on-plate tests were made by the gas tungsten-arc process and by high and low voltage electron beam processes. The heat input and weld nugget area were varied, and the effect of grain size, segregation, silicon and manganese content, and nugget shape on microcracking were investigated.

A mechanism of heat-affected zone microcracking has been developed from this investigation. It suggests that the cracking is caused by the combined factors of weld shape, grain size, and the presence of a weak phase in the grain boundary at the temperature at which cracking occurs.

The first workable models of the aircraft gas turbine engine were developed by Whittle<sup>1</sup> in 1939 and 1940. The efficiency of the prototype engine depended mainly upon the temperature of the gases after combustion. This, of course, meant that the turbine blades and rotor would be required to withstand high temperatures plus large induced stresses. Thus, to accommodate this need, the development of high-temperature, high-strength superalloy materials began.

## Introduction

Alloy 718 is a high strength precipitation hardened alloy which is used in

the temperature range of -423 to 1300° F (-250 to 700° C). The nominal composition of this alloy is shown in Table 1. Some physical and mechanical properties are listed in Table 2. Alloy 718 is hardened by a precipitate which is coherent with the matrix. The precipitant is body centered tetragonal Ni<sub>3</sub> (Cb, Ti, Al) with the columbium being most abundant.<sup>2</sup> This structure is called gamma prime, and is different from most precipitation-hardening constituents which are face centered cubic. Upon overaging the gamma prime transforms into the stable orthorhombic form of Ni<sub>3</sub> (Cb, Ti, Al).

The major difference between this alloy and other nickel-base alloys is the sluggishness of the gamma prime reaction. The delayed gamma prime formation makes alloy 718 ideal for welding; the reaction is slow enough that the transformation is delayed sufficiently for stress relief to occur before much aging is achieved, during the postweld aging treatment. In this

M. J. LUCAS, JR., is with the Research Division, Babcock and Wilcox Co., Alliance, Ohio and C. E. JACKSON is Associate Professor, Department of Welding Engineering, The Ohio State University, Columbus, Ohio.

Paper presented at the AWS 50th Annual Meeting held in Philadelphia, Pa., during April 26 to May 2, 1969.

**Table 1—Chemical Composition of Alloy 718**

|                 | Composition, % <sup>b</sup> |               |
|-----------------|-----------------------------|---------------|
|                 | Wrought                     | Cast          |
| Cr              | 17.00 -21.00%               | 17.00 -21.00% |
| Mo              | 2.80 - 3.30                 | 2.00 - 4.00   |
| C               | 0.03 - 0.10                 | 0.10          |
| Co <sup>a</sup> | 1.00                        | —             |
| Ni              | —                           | 50.00 -55.00  |
| Ni + Co         | 50.00 -55.00                | —             |
| Cb + Ta         | 5.00 - 5.50                 | 4.50 - 7.00   |
| Al              | 0.40 - 0.80                 | 0.20 - 1.00   |
| Si              | 0.35                        | 0.75          |
| P               | 0.015                       | —             |
| S               | 0.015                       | 0.03          |
| B               | 0.002- 0.006                | —             |
| Cu              | 0.10                        | 0.75          |
| Mn              | 0.35                        | 0.50          |
| Ti              | 0.70 - 1.15                 | 0.20 - 1.30   |
| Fe              | Balance (16%)               | Balance (16%) |

<sup>a</sup> If determined.

<sup>b</sup> Single values are maximum.

**Table 2—Properties of Alloy 718 in Cast Form**

| Test temperature, °F             | Tensile strength, kpsi | Yield strength (0.2% offset), kpsi | Elongation in 1 in., % | Reduction of area, %       |      |
|----------------------------------|------------------------|------------------------------------|------------------------|----------------------------|------|
|                                  |                        |                                    |                        |                            | °C   |
| Room                             | Room                   | 152.3                              | 116.9                  | 25.4                       | 24.7 |
| 600                              | 316                    | 133.3                              | 107.7                  | 27.5                       | 31.1 |
| 800                              | 427                    | 125.1                              | 102.9                  | 28.2                       | 27.7 |
| 1000                             | 537                    | 121.1                              | 98.6                   | 27.3                       | 33.7 |
| 1200                             | 649                    | 125.5                              | 103.5                  | 19.3                       | 31.8 |
| 1350                             | 732                    | 109.5                              | 93.1                   | 11.4                       | 19.8 |
| 1400                             | 760                    | 98.8                               | 84.3                   | 8.7                        | 10.8 |
| 1450                             | 788                    | 94.1                               | 77.2                   | 8.5                        | 9.8  |
| 1600                             | 871                    | 49.4                               | 32.6                   | 27.3                       | 45.2 |
| Physical properties <sup>a</sup> |                        | Temperature, °C                    |                        | Units                      |      |
| Density                          |                        | 22                                 |                        | 8.23 grams/cm <sup>3</sup> |      |
| Electrical resistivity           |                        | 22                                 |                        | 121 microhm-cm             |      |
| Coefficient of thermal expansion |                        | 22-93                              |                        | 12.78 microns/m/°C         |      |
|                                  |                        | 24-204                             |                        | 13.50 microns/m/°C         |      |
|                                  |                        | 24-316                             |                        | 13.85 microns/m/°C         |      |
|                                  |                        | 24-427                             |                        | 14.23 microns/m/°C         |      |
|                                  |                        | 24-538                             |                        | 14.40 microns/m/°C         |      |
|                                  |                        | 24-649                             |                        | 15.12 microns/m/°C         |      |
|                                  |                        | 24-760                             |                        | 16.03 microns/m/°C         |      |

<sup>a</sup> Aged condition

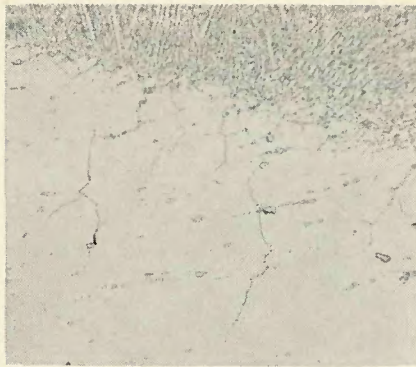


Fig. 1—Typical photomicrograph of the microcracking in the heat-affected zone of electron beam welds on alloy 718.  $H_3PO_4$  etch.  $\times 200$  (reduced 50% on reproduction)

manner, postweld strain age cracking problems are minimized. However, Alloy 718 is not free of welding problems, as one of the most critical problems is the formation of heat-affected zone microcracks during electron beam welding. These cracks are intergranular and of the order of a few mils in length. In normal application, such as in rocket or jet engines, these little fissures may grow and have deleterious effects. A typical condition is shown in Fig. 1.

### Objective

The objective of this program was to study the response of alloy 718 to gas tungsten-arc and electron beam welding; the heat-affected zone was examined as to its hardness, structural phases present, grain size and microcracking tendency. An attempt was made to develop a theory for the mechanism of cracking and to point out those factors which influence the heat affected zone microcracking in alloy 718.

### Experimental Procedure

A number of heats from which material was available, shown in Table 3, provided a range of composition for the welding study. These heats were examined for their cracking tendency, grain size, and the influence of

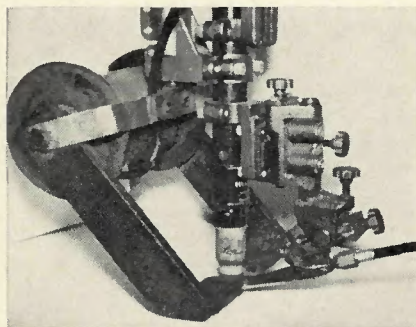


Fig. 2—Welding equipment used in the investigation. Note electromagnet for magnetic study

Table 3—Compositions of the Heats of Alloy 718 Used in the Investigation, Wt-%

| Heat number | Composition by heat numbers, wt-% |         |                   |                   |                   |                   |
|-------------|-----------------------------------|---------|-------------------|-------------------|-------------------|-------------------|
|             | 1958                              | 9186    | MJL1              | MJL2              | MJL3              | MJL4              |
| Cr          | 19.27                             | 18.70   | 19.36             | 19.49             | 19.17             | 19.76             |
| Mo          | 3.20                              | 3.23    | 3.00              | 2.43              | 3.00              | 2.96              |
| C           | 0.07                              | 0.07    | 0.03              | 0.03              | 0.04              | 0.04              |
| Co          | 0.38                              | 0.19    | 0.07              | 0.15              | 0.64              | 0.28              |
| Ni          | 53.87                             | 52.94   | 53.06             | 53.20             | 53.72             | 53.50             |
| Cb + Ta     | 5.10                              | 5.42    | 3.03 <sup>a</sup> | 5.10              | 5.01              | 5.13              |
| Al          | 0.61                              | 0.62    | 0.99 <sup>b</sup> | 1.05 <sup>a</sup> | 0.95 <sup>b</sup> | 1.05 <sup>b</sup> |
| Si          | 0.04                              | 0.02    | 0.03              | 0.36              | 0.01              | 0.35              |
| P           | 0.003                             | 0.002   | 0.002             | 0.002             | 0.003             | 0.003             |
| S           | 0.006                             | 0.005   | 0.003             | 0.002             | 0.001             | 0.001             |
| B           | 0.004                             | 0.003   | 0.003             | 0.006             | 0.005             | 0.006             |
| Cu          | .01                               | .01     | .001              | .01               | .01               | .01               |
| Ti          | 0.85                              | 0.88    | 0.66 <sup>a</sup> | 0.25 <sup>a</sup> | 0.33 <sup>a</sup> | 0.43 <sup>a</sup> |
| Mn          | 0.01                              | 0.10    | 0.15              | 0.19              | 0.05              | 0.26              |
| Fe          | 16.40                             | Balance | 19.40             | Balance           | Balance           | Balance           |

<sup>a</sup> Less than alloy 718 specification.

<sup>b</sup> Higher than alloy 718 specification.

microstructure, variations in composition, metallographic phases which are present and hardness changes. A brief review of the possibility of stress being a factor in the cracking found in this material was made.

Both gas tungsten-arc and electron beam welding were available and used to provide a wide range of conditions for studying the mechanism of fissuring of the heat-affected zone during welding.

### Welding Procedure and Equipment

The gas tungsten-arc welding equipment used in this program is shown in Fig. 2. This was a 500 amp commercial unit. Tungsten electrodes, (1% thoriated), 3/16 in. in diameter, and grade A helium and argon were used during welding. Electronic governors were used to regulate both travel of the carriage and the wire feeder. An electro-magnet shown in Fig. 2 was used for the magnetic field series of welds. Welding current was continuously recorded on a graphic recorder. The voltage was registered on a calibrated voltmeter.

### Gas Tungsten-Arc Welds

The gas tungsten-arc weldments

made for this program were in four series:

*Series 1—Preliminary Tests.* The first series consisted of 300 bead-on-plate weldments with varying welding parameters in order to see if the process would cause microcracking similar to that reported for the electron beam welding process. The plates were ground prior to welding to remove any contamination on the surface. The gas tungsten-arc welds were made using currents from 100 to 700 amp with dcsp and 14 to 41 v with the speed of travel from 8 to 120 ipm. The material for all of the welds was 3/8 in. thick solution annealed plate.

The welds were sectioned and prepared for metallographic inspection for fissuring. Some of the specimens were studied further using the microprobe and microhardness testing equipment. Microcracks were found only in those welds which exhibited undercutting.

*Series 2—Grain Size Study.* The second series of weldments were used for a study of the effect of grain size on the cracking tendency of the alloy. The plates used were specially prepared pieces which exhibited fine

Table 4—Schedule for Producing Material for Grain Size-Structure Experiment

| Solution temperature | Grain size  |      |    |     |   |      |      |      |
|----------------------|---|------|----|-----|---|------|------|------|
|                      | Fine (~5)   |      |    |     | Coarse (~3)   |      |      |      |
|                      | Heat at A° F/1 hr. Hot roll at A° F with two or more passes totaling B% each. Air cool to room temperature. Start with C in. material. Finish size is D in. |      |    |     | Heat at E° F/1 hr. Air cool; then reheat to F° F for G hr. Use 1/2 in. material |      |      |      |
| °F                   | °C  | A    | B  | C   | D   | E    | F    | G    |
| 1750                 | 954   | 1750 | 33 | 3/4 | 1/2   | 2050 | 1750 | 24.0 |
| 1850                 | 1010  | 1850 | 33 | 3/4 | 1/2   | 2050 | 1850 | 15.0 |
| 1950                 | 1066  | 1950 | 50 | 1   | 1/2   | 2050 | 1950 | 10.0 |
| 2050                 | 1121  | 2050 | 50 | 1   | 1/2   | 2050 | 2050 | 5.0  |

and coarse grain microstructures at a given solution annealed temperature—Table 4. The effect of both grain size and phase structure could be evaluated by sectioning. The weldments were sectioned and the cross-sections polished. The heat-affected zone was checked for micro-cracking by both visual and fluorescent penetrant inspection.

**Series 3—Liquid Nitrogen Cooled Plates.** Since under normal welding conditions (those which produce no undercutting) the cracking occurred mainly with electron beam welding, it was thought that maybe the quenching action of the electron beam process contributes to the cracking tendency. To increase the quenching rate of the gas tungsten-arc welds, the plates were cooled in liquid nitrogen immediately prior to welding. The parameters used were varied from known good conditions to those which were microfissure prone. The welds were examined both visually and with fluorescent penetrant for heat-affected zone cracks.

**Series 4—Special Heat-Treatment Plates.** Since the preliminary studies showed hot cracks in the partially melted region of the heat-affected zone, simulated specimens were prepared in order to study this phenomenon. Pieces were heated in a furnace at 25° F (14° C) intervals from 2175 to 2400° F (1191 to 1316° C). It was found that at approximately 2325° F (1274° C) the grain boundaries began to fuse. This condition would tend to promote microcracking. Since simulated samples were larger than the heat-affected

zone adjacent to a weld deposit, they were satisfactory for study by the microprobe.

If the grain boundary condition was a primary cause for cracking, susceptibility of the alloy to microcracking should increase if the condition existed prior to welding. Therefore, two plates were heated to 2350° F (1288° C) and held for 15 min before air cooling. These plates were then ground and welds made on the surface. Two of the welds were made with the magnetic field superimposed upon the arc in order to change the weld shape, since the shape of the weld may also be a contributing factor in the microcracking condition. Welding speed was increased to the maximum in order to provide a condition which showed satisfactory welds and no undercutting and welds with unsatisfactory contour because of undercutting.

#### Electron Beam Welds

Electron beam welds were made with both high voltage and low voltage equipment in order to determine if there was any difference in cracking susceptibility with either technique. A series of over 100 welds was made with the voltages in the high range between 100 and 150 kv at 10 to 15 milliamp and 5 to 60 ipm travel. With the low voltage equipment, the range was 22 to 26 kv at 110 to 155 milliamp and 20 to 45 ipm travel. The comparison welds for these two machines were made on plates solution annealed at 1950° F for 1 hr. These welds were inspected by visual and fluorescent penetrant for microcracks.

The next series of weldments was made to investigate the effect of grain size on the cracking tendency. The welds were made on pieces of the same material as used for the gas tungsten-arc evaluation. Welds were made with both the high voltage and the low voltage machines. Also, a special heat of material produced with a very fine grain size (ASTM 10) was welded with the low voltage unit.

The third series of welds was made on aged and overaged material. Three standard aging treatments and one overage treatment were used for four plates which were welded in this series. The aging treatments are described in Table 5. The overaged sample was produced by heating at 1550° F (843° C) for 1 hr after solution annealing at 1750° F. Previous tests performed on small specimens indicated that this material overaged in 15 min at this temperature. The larger piece was heated for 1 hr to ensure that the entire plate had reached the desired temperature for the minimum of 15 min.

An additional series of materials was prepared with a range of manganese and silicon content in order to determine the effect of these elements on the cracking resistance of alloy 718. These were prepared since Morrison and his co-workers<sup>3</sup> have reported high manganese and high silicon increase the cracking resistance of alloy 718. The results of this series are listed in Table 6.

#### Welding Parameters

The welds made using the low voltage electron beam equipment and the sections were examined by visual and fluorescent penetrant for heat-affected zone microcracking. Additional tests were made in order to provide a means for setting up techniques that were needed in the laboratory approach. The parameters used in making these welds with low voltage electron beam are listed in Table 7. The results of the investigation, shown graphically in Fig. 3, indicates the number of heat-affected zone cracks which were found. This material had been solution annealed at 1750° F (954° C). The variation in welding

Table 5—Aging Treatment for Alloy 718

| Solution heat treatment       | Aging treatment <sup>a</sup>  |
|-------------------------------|---|
| 1750° F (954° C), rapid cool  | 1750° or 1700° F (954 or 927° C) for 1 hr., air cool.<br>1325° F (718° C) for 8 hr., furnace cool to 1150° F (621° C) and hold until a total of 18 hr. have elapsed, air cool |
| 1800° F (982° C), rapid cool  | 1325° F (720° C) for 8 hr. furnace cool to 1150° F (621° C) and hold until a total of 18 hr. have elapsed, air cool   |
| 1950° F (1066° C), rapid cool | 1350° F (732° C) for 8 hrs. or 1400° F (760° C) for 10 hr. furnace cool to 1200° F (649° C) and hold until a total of 20 hr. have elapsed, air cool                           |

<sup>a</sup> Overaged sample produced by heating at 1550° F (843° C) for 1 hr after an annealing solution heat-treatment at 1750° F (954° C).

Table 6—Effect of Manganese and Silicon Content on Microcracking of Alloy 718<sup>a</sup>

| Mn, % | Si, % | Degree of weld cracking <sup>b</sup><br>under four different welding conditions |          |          |          |
|-------|-------|---|----------|----------|----------|
|       |       | 1   | 2        | 3        | 4        |
| 0.15  | 0.03  | Fair  | Fair     | Fair     | Fair     |
| 0.36  | 0.19  | Very Bad  | Very Bad | Very Bad | Very Bad |
| 0.05  | 0.01  | Bad   | Fair     | Fair     | Fair     |
| 0.26  | 0.35  | Very Bad  | Very Bad | Very Bad | Very Bad |

<sup>a</sup> Base metal annealed at 1750° F (954° C)

<sup>b</sup> All welds cracked.

Table 7—Parameters of Electron Beam Welds Used for Studying the Cracking Problems of Alloy 718

| Weld<br>Travel<br>num-<br>ber | Speed,<br>ipm | Voltage,<br>kv | Current,<br>millamp | Gun-to-                |
|-------------------------------|---------------|----------------|---------------------|------------------------|
|                               |               |                |                     | work<br>height,<br>in. |
| HSA                           | 51            | 26             | 155                 | 1.75                   |
| HSB                           | 51            | 22             | 120                 | 1.75                   |
| HSD                           | 45            | 22             | 122                 | 1.75                   |
| HSL                           | 45            | 25             | 137                 | 1.75                   |

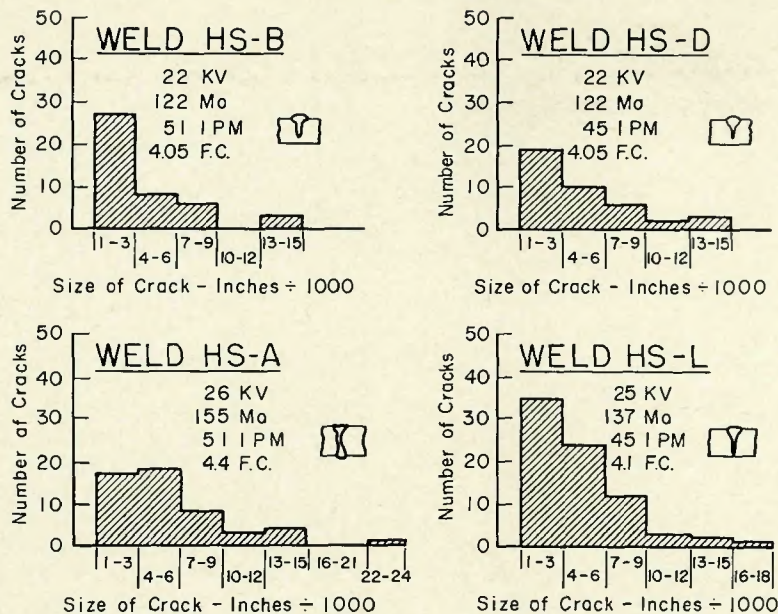


Fig. 3—Number of cracks as a function of crack length for four different electron beam welds on solution annealed alloy 718

parameters had very little effect on the microcracking tendencies of this particular sample.

The shape of the welds also is illustrated in Fig. 3. Microcracks extend from the edge of the fusion zone into the heat-affected zone. At high magnification it appears that the grain boundary began to melt during the welding operation. The majority of the cracks were located at the bottom of the nail head of the weld metal just before it changes to the spike of the weld. The majority of the intergranular cracks were less than 0.006 in. (0.15 mm) in length.

Changes in the welding parameters did not have any marked effect on the cracking tendency of the alloy. Selected samples from each series of weldments were investigated further with Knoop hardness measurements, stress studies, and electron microprobe measurements.

## Results

The results include both the gas tungsten-arc and electron beam welds under each subheading. In this way a

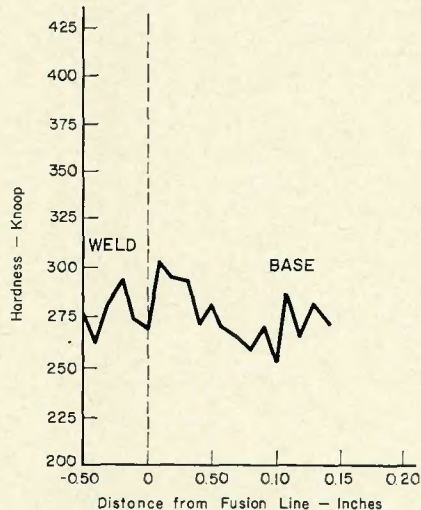


Fig. 5—Knoop hardness survey of weld on overaged alloy 718

major emphasis can be placed on the mechanism of microfissuring rather than the welding techniques. Since welding technique is not a major factor, it was hoped that a better background would be provided with this

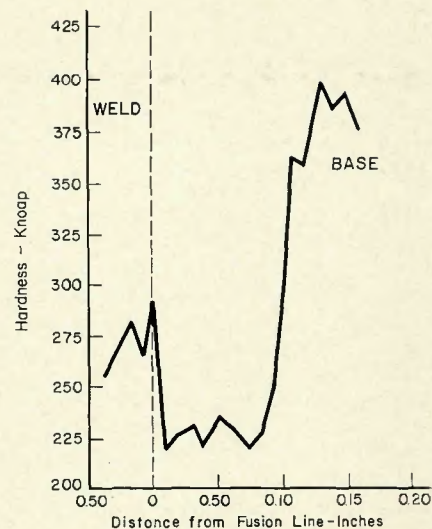


Fig. 4—Knoop hardness survey of weld on aged alloy 718

approach. A number of specimens were studied in order to determine whether there was any extreme hardening taking place in the heat-affected zone. No correlation could be found between hardness and the cracking tendency.

Plots for measurements taken on welds on aged and overaged material are shown in Figs. 4 and 5 respectively. Figure 4 shows a softening of the metal in the heat-affected zone due to the welding which annealed the region next to the weld. Figure 5 shows the normal response to the welding thermal cycle. The change in welding parameters did not show any signs of influencing the cracking tendency of alloy 718 in the range studied.

## Microscopic Examination

Upon polishing the samples, the microstructure revealed that there was a tendency for melting of the grain boundaries near the fusion line. Figure 6 shows the grain boundary thickening near the fusion line for a weld made by the gas tungsten-arc process. Grain boundary segregation or liquation is evident in the weldments shown in Fig. 7.

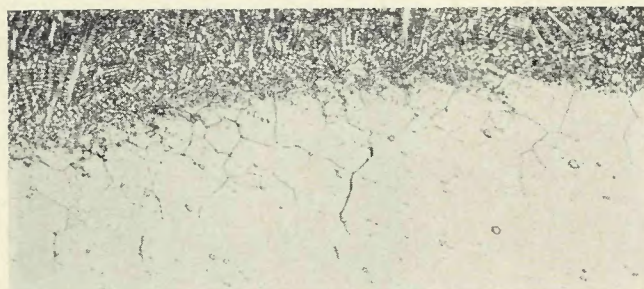


Fig. 6—Photomicrograph of gas tungsten-arc weld showing segregation at the grain boundaries near the fusion line.  $H_3PO_4$  etch.  $\times 200$  (reduced 35% on reproduction)

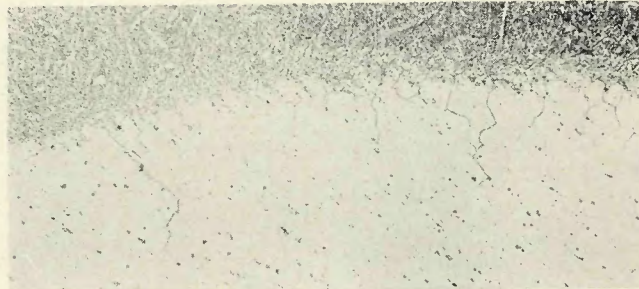


Fig. 7—Photomicrograph of gas tungsten-arc welded specimen showing segregation at the grain boundaries near the fusion line.  $H_3PO_4$  etch.  $\times 100$  (reduced 35% on reproduction)

The micrograph of an electron beam weld shown in Fig. 8 indicates the same type of condition but to a lesser degree than that obtained with the gas tungsten-arc welds.

### Special Heat Treatment

Since the area adjacent to the fusion line in the heat-affected-zone appeared to be segregated at the boundaries, a study of the incipient melting behavior of the material was undertaken. Figure 9 shows the change in microstructure of the material as it is heated from 2275 to 2408° F (1246 to 1320° C). This type of grain boundary melting is most likely the reason for heavy grain boundaries adjacent to the fusion line in the heat-affected zone.

All welds made on plates annealed at 2350° F (1288° C) for 15 min indicate cracking condition. The cracking occurred at welding conditions which were not crack-sensitive with the proper solution annealed plate. Since the grain boundary condition increased the cracking susceptibility of alloy 718, it is suggested that a microstructural phase forms in the grain boundaries during the welding process; this has insufficient strength at the time stresses are applied to it by the welding operation.

### Microprobe Experiments

Two gas tungsten-arc welds were studied with the electron microprobe technique. Figure 10 shows the areas which were scanned. The precipitates occurring at the grain boundaries were rich in columbium, and titanium

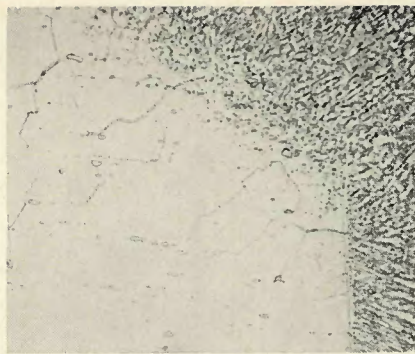


Fig. 8—Photomicrograph of electron beam welded specimen showing segregation at the grain boundaries near the fusion line.  $H_3PO_4$  etch.  $\times 200$  (reduced 50% on reproduction)

with a high carbon content associated with a decrease in nickel, chromium and iron. The area was so small that the results may not have revealed all of the constituents in the grain boundaries.

The 2361 and 2408° F (1294 and 1320° C) special heat-treated samples have broad grain boundaries which are ideal for the microprobe study. Identical results were obtained for both of these samples; the microprobe indicated a decrease in chromium, iron and nickel content with an increase in columbium and carbon at the grain boundaries. There appeared to be no change in the content for manganese, silicon, aluminum and titanium. These results agree with those found by Morrison and his co-workers.<sup>3</sup>

### Grain Size Solution Temperature

The grain size solution temperature

study produced very useful data in determining the effect of grain size on cracking. In the gas tungsten-arc welding series, all of the welds on the coarse grained plate cracked and also all the fine grained welds except those on the 1850° F (1010° C) solution-annealed plate cracked. The cracks on the coarse grained material were much larger than those in the fine grained materials. All of the welds had an unfavorable undercut shape which promoted cracking; this was caused by welding at excessively high travel speeds.

The results for electron beam welds are more decisive than the gas tungsten-arc welds. Welds made on the high voltage machine showed no cracks on the fine grained materials, while at least one weld on each of the coarse grained material cracked. Welds made by the low voltage electron beam process on the reference heat (1958) of alloy 718 showed microcracks with all specimens having moderately large grain size. The extremely fine grained material (ASTM 10) showed no cracking in the heat-affected zone. Figure 11 shows a micrograph of an electron beam weld in this special material.

### Effect of Manganese and Silicon

The special heats of alloy 718 with the varied amounts of manganese and silicon all showed cracks. The plates with the high manganese and silicon content showed the greatest cracking tendency of the plates tested. The plates with the high manganese but low silicon did not crack as badly as most of the specimens tested. The

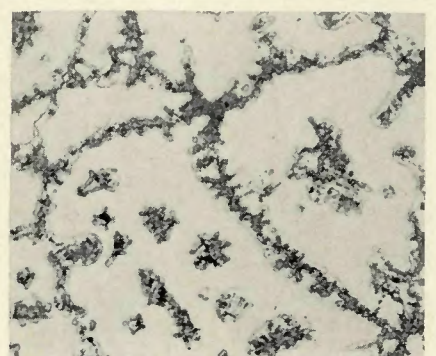
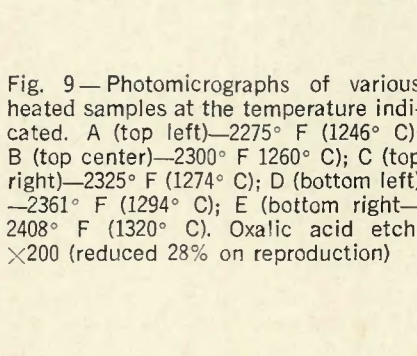
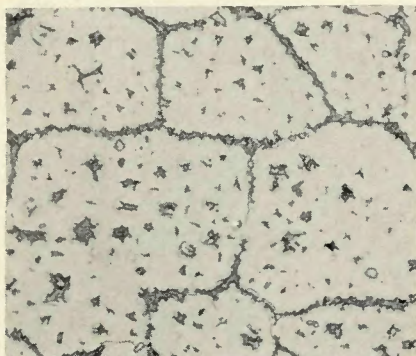
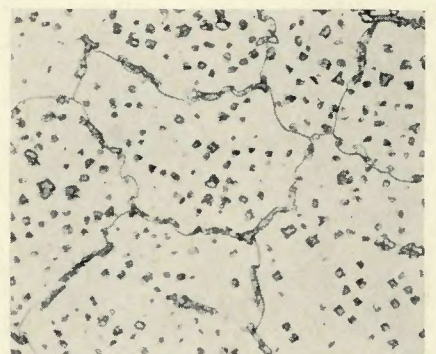
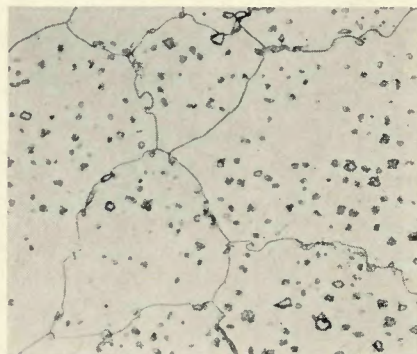
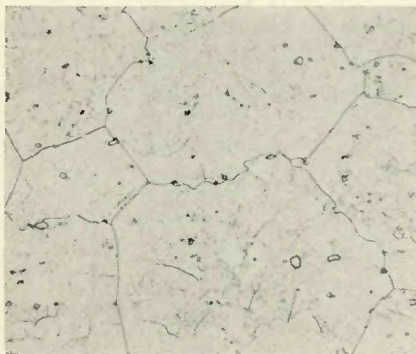


Fig. 9—Photomicrographs of various heated samples at the temperature indicated. A (top left)—2275° F (1246° C); B (top center)—2300° F (1260° C); C (top right)—2325° F (1274° C); D (bottom left)—2361° F (1294° C); E (bottom right)—2408° F (1320° C). Oxalic acid etch.  $\times 200$  (reduced 28% on reproduction)

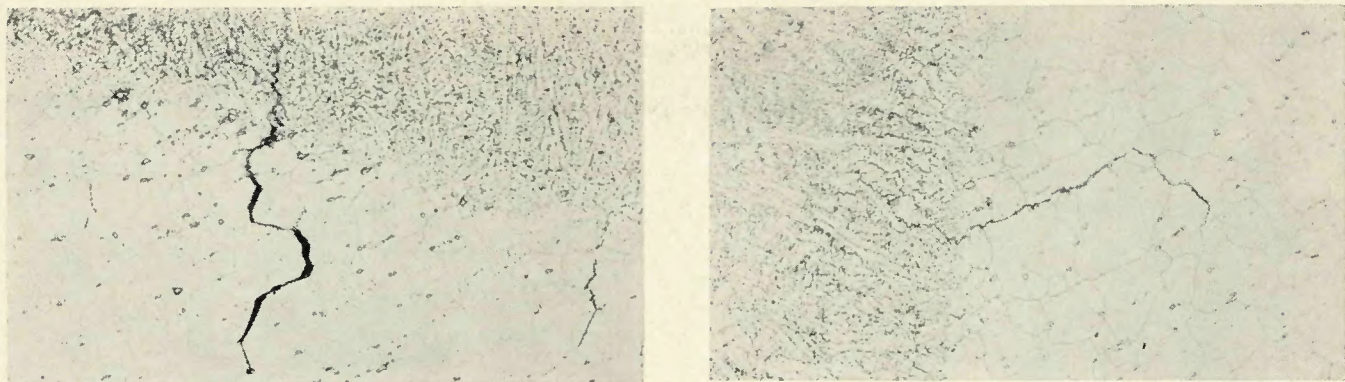


Fig. 10—Area of two gas tungsten-arc welds in alloy 718 which was analyzed by the microprobe. Oxalic acid etch.  $\times 100$  (reduced 35% on reproduction)

plate with low silicon and manganese cracked similar to the reference heat of alloy 718 used throughout the program—Table 6.

#### Heat Treatment

Heat treatment had little effect on reducing the microcracking tendency of alloy 718. All of the material evaluated cracked, but the aged samples had more cracks than any other condition. The aging treatment produced progressively more crack-sensitive material as the solution temperature associated with the aging treatment increased. The results show that the higher the solution temperature, the greater the cracking tendency, confirming the results reported by previous investigators.<sup>3,4</sup> The nitrogen cooled plates, overaged plates, and preheated plates behaved in a manner similar to the 1950° F (1066° C) solution-annealed plates used for the majority of this program.

In general, it is noted that the use of normal heat-treating practices with alloy 718 showed little effect on reducing the cracking tendency of the weld heat-affected zone.

#### Stress Analysis

Since the grain size of the alloy is very large and the X-ray spot is very small, examining the heat-affected zone of alloy 718 with this technique,

was not satisfactory. Insufficient grains could be sampled to adjust to the distribution of preferred crystal orientation which even a high temperature anneal did not remove. No satisfactory results were obtained in attempting to use special X-ray measurements on alloy 718.

Since it was the object of this stress measurement approach to determine whether a stress distribution was influenced by the shape of the weld nugget, another material was selected in order to obtain supplementary data in this field. Weldments were made on Type 410 stainless steel which could be studied by the X-ray diffraction equipment.<sup>5</sup> The tests indicated that the stresses are probably higher in the area where the weld changes shape (Fig. 12), since the majority of the cracking occurs in this area.

Since the X-rays average spot size is a large area of the heat-affected zone, an analysis of the area adjacent to the fusion line is very difficult. Hence, X-ray examination using the diffraction technique for measuring the stress level in the gas tungsten-arc welds did not provide reliable values. The fact that the gas tungsten-arc weld had a stress level which was lowest midway from the top of the weld and the bottom is probably of no consequence.

#### Magnetic Fields

A magnetic field<sup>6</sup> was applied to the arc to modify the shape of the weld nugget. The magnetic field made it possible to increase the speed to 45 ipm without any undercutting effect. At this point a limit of the technique was obtained, and any increase in the magnetic field made the arc unstable which increased the undercutting tendency.

Two gas tungsten-arc welds were made at the maximum speed of 45 ipm and cross sectioned—Fig. 13. One weld had a satisfactory bead contour and showed no cracking. The second was undercut and cracked in the

region where the weld shape changed. Thus, since the only parameter change in this series was weld shape, it is felt that the weld nugget shape contributes to the cracking tendency of the alloy. This verifies the results that only the undercut gas tungsten-arc welds cracked.

#### Discussion

The experimental tests of this program were directed towards a description of a mechanism of hot cracking in the heat-affected-zone of alloy 718. The approach was to study the changes in the microstructure in the heat-affected zone and relate these changes with the cracking problem. The effect of bead shape and stress distribution was considered in order to determine whether these factors influence the cracking susceptibility of alloy 718. The discussion section attempts to give a description of what happens in the heat-affected zone of alloy 718. Finally, a mechanism describing the hot cracking tendency will be proposed.

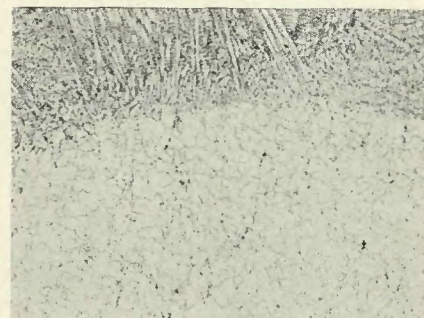


Fig. 11—Photomicrograph of electron beam weld HS2 in alloy 718 which has an extremely fine grain size. Oxalic acid etch.  $\times 200$  (reduced 50% on reproduction)

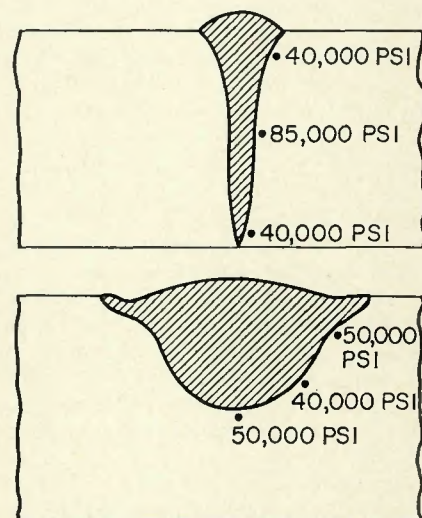


Fig. 12—Results of X-ray diffraction stress analysis of Type 410 stainless steel. A (top)—electron beam weld; B (bottom)—gas tungsten-arc weld

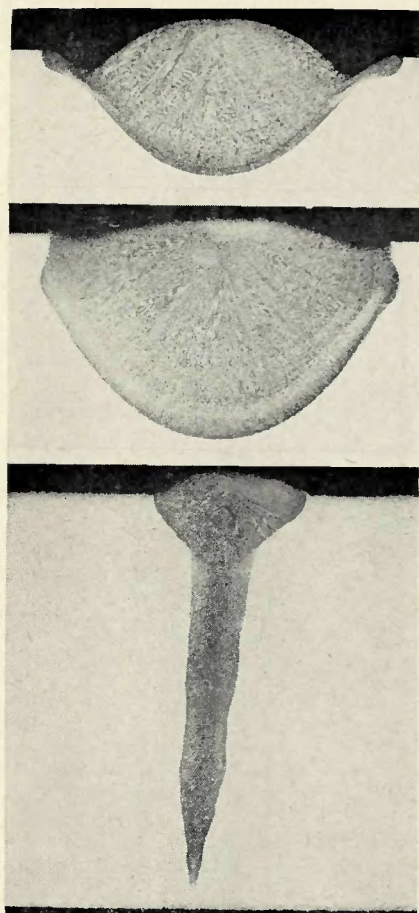


Fig. 13—Typical macrographs of the cross section of welds made during this study.  $H_2PO_4$  etch.  $\times 10$  (reduced 35% on reproduction)

#### Stress Analysis

Since alloy 718 did not lend itself to study by the X-ray diffraction method a Type 410 stainless steel was selected. Precise location of the beam was not possible, and the stress level of the area just adjacent to the fusion line could not be measured. As the X-ray spot was approximately 1 mm in diameter, it was not possible to observe the area next to the fusion line which was in the order of 0.1 mm. Consequently, the area being studied by X-ray diffraction was an average of the area close to the fusion line in the heat-affected zone. High stresses were located throughout the area and the actual stress at the point of cracking may be higher than the average measured by X-ray diffraction.

Referring to Fig. 12, it must be noted that cracking will take place at a temperature just below the melting temperature of the alloy. If conditions are right, a very small stress could cause fracture at these temperatures. The areas next to the weld metal at a high temperature supported by the adjacent cool material could well develop stresses of sufficient magnitude to cause fracture.

The majority of the cracks in the

specimens examined were located where the weld nugget changes shape. Only the welds on the special composition heats produced cracks in locations other than where the weld nugget changed shape. If the cracking was entirely caused by metallurgical disturbances, the probability of their occurrence at any point along the weld would be nearly the same. It is recognized that the presence of this geometrical change may be the cause of metallurgical changes in the heat-affected-zone.

Further proof of the effect of weld shape on cracking was demonstrated in the tests with the magnetic field across the arc. The normal welding conditions which produced cracks did not produce cracks when the magnetic field was used. The magnetic field removed the undercut and subsequent drastic change in nugget shape. Weld shape appears to be a major factor in the cracking susceptibility of weldments in alloy 718.

#### Heat Treatment-Hardness-Grain Size

The heat treatment which the material received before welding had a slight effect on the cracking susceptibility of alloy 718. None of the heat treatments decreased the cracking tendency from that of the 1750° F solution-annealed material. The cracking susceptibility increased for the aged material which became more crack-sensitive as the solution temperature was increased. The increase in grain size which is associated with increased solution temperature may be the important factor. The aged structure appears to be more crack-sensitive than the annealed material since the heat-affected zone is subjected to structural changes with a different stress pattern during welding. The heat-affected

zone of the aged material is most likely solution-annealed, because its hardness is nearly identical with the hardness of the solution annealed plate.

The investigation showed that the fine grained material is less crack-sensitive than coarse grained material. A logical explanation can account for this behavior, since as the grain size increases the surface area of grain boundary per unit volume decreases rapidly. If something is forming in the grain boundaries, there will be a larger amount per unit area in the coarse grained material than the fine grained since the segregate is spread over less area. Also, as the grains grow to a large size the boundaries trap impurities which tend to lower the melting point of that region. Since more foreign particles are introduced into the grain boundary as the grain size increases, the melting point of the grain boundary is decreased. Thus, the coarse grained material would be more sensitive to welding stresses than the fine grained material.

#### Composition—Manganese and Silicon Content

The chemical composition has an effect on the cracking susceptibility of alloy 718. The results of the manganese-silicon content show that the cracking susceptibility of the alloy increases as the amount of these elements in the alloy increases. The heat made with the high silicon and high manganese content produced cracks all along the fusion line of the electron beam welds. No other plate cracked this extensively. The other plates which had a large amount of manganese or silicon also cracked much more than the standard heat of alloy

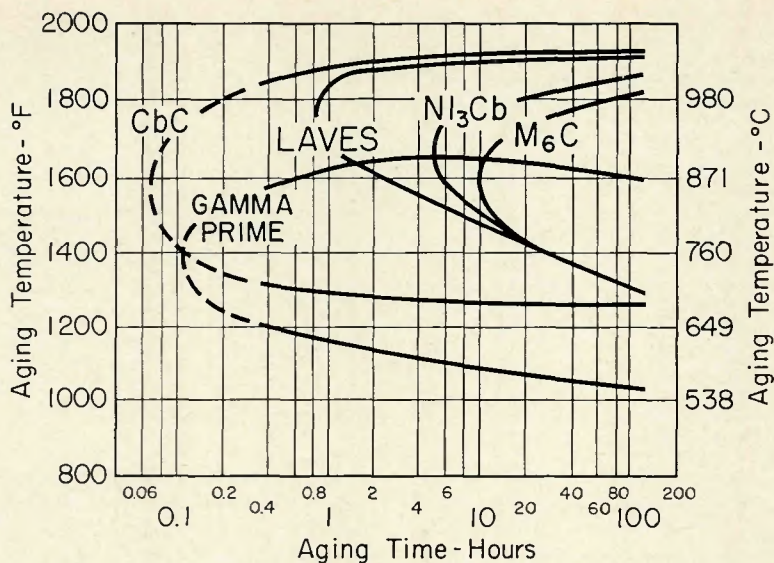


Fig. 14—Time-temperature-transformation diagram for alloy 718 after annealing at 2100° F for 1 hr and water quenched

The change in the structure near the bond line is due to grain growth and grain boundary changes which occur in this region. A gradient for the diffusion of atoms into the grain boundaries makes it possible for new phases to form on solidification. It is believed that this phase is columbium carbide. The time-temperature-transformation diagram (Fig. 14) indicates that columbium carbide (CbC) is the first phase to form during cooling.<sup>7</sup> Therefore, the formation of columbium carbide is expected if the conditions are favorable for these phase changes.

Columbium carbide is a brittle material which forms very readily when columbium and carbon are present ( $H^{\circ}298 = -33.6$  kcal/mole). The carbide has a hardness of Rockwell A 91 with a strength of 35,000 psi at 2000° C. The carbide appears to be a grain boundary film instead of a globular precipitate; if a crack forms in this film, it will run for some distance before arresting itself.

The region which contains columbium carbide is believed to be partially responsible for the microcracking in alloy 718. A stress must also be present to cause cracking to occur. A decrease in grain size increases the total surface of the grain. The impurities at the grain boundary are reduced from those of the coarse grained material, because of the increase in surface of the grain boundary constituent per unit volume.

### Proposed Mechanism of Hot Cracking in Alloy 718

The results of the investigation show that several changes occur in the heat-affected zone of alloy 718. These changes are related to the hot cracking which occurs in this alloy. The main contributing factors are grain boundary carbides, grain size, and geometric shape of the weld nugget. These are all interrelated as previously discussed. A mechanism of cracking can be proposed which combines some of the present proposed theories.

At high temperatures near its melting point the material has very little strength and ductility. If stresses are applied to a region during this temperature range, the material will fracture quite easily. At these high temperatures with the incipient melting, the susceptibility for cracking is increased. This increase is due to the fact that the stress pattern can upset the solid mass in the area and when the metal cools, insufficient liquid will be available to fill the entire volume. Thus, a crack due to shrinkage or hot tearing will occur. At these high temperatures the matrix supports little of

the load applied to it. The grain boundaries are forced to support the load which usually results in shearing or deformation. If the shearing occurs at a junction of three grains, a void may develop which can grow by continued sliding of the boundary. This has been described by Zener<sup>8</sup> in his proposed mechanism for hot cracking.

At the high temperatures involved, diffusion is very high. The atoms can move quite easily through the lattice because of the high energy of the atoms at such temperatures. In a liquid, diffusion is very rapid. In the case of melting at the grain boundaries adjacent to the molten weld nugget, elements and compounds in the molten nugget can mix with the molten grain boundary which results in a new composition of the grain boundary upon solidification. Thus, liquid diffusion can be a source of obtaining high concentrations of some elements, say carbon, during welding. All of the factors discussed here have some effect on the hot cracking susceptibility of alloy 718.

The following is proposed as a mechanism of cracking of alloy 718. When the heat of the welding arc or electron beam strikes the surface of the material, a weld nugget is rapidly formed. The heat causes grain boundary changes to occur in the heat-affected zone adjacent to the bond line. The heat also causes the base metal to expand putting grains in compression during heating. On the other hand, as the weld metal begins to solidify the metal in the weld contracts with a decrease in temperature. However, the contraction is restrained by the cold base metal. The area just adjacent to the fusion line undergoes plastic deformation and further contraction increases the tension forces. As this is taking place, the grain boundaries which contain the columbium carbide film begin to solidify. Since the temperature is still very high and the strength of the carbide film is low, little stress is required to fracture these areas.

It is believed the shape of the weld nugget can increase the stress in the weld heat-affected zone. The stress caused by the shrinking weld metal is parallel to the bond line. Where the shape changes, these stresses tend to be perpendicular to one another. The shear stresses in this area are probably intensified due to the action of the two perpendicular forces.

Another factor contributing to the cracking, but to a lesser degree is the pile up of dislocations. The columbium carbide precipitate in the grain boundaries restricts the movement and a moderate stress may build up which causes fracture of the carbide film. It

appears columbium must be present in the alloy for cracking to occur; columbium may form a low melting point constituent which is not formed when this element is removed.<sup>9</sup>

### Remedies

The cracking condition can be alleviated by reducing the grain size and making welds with a smooth nugget shape. The first remedy is very difficult to do with this type of alloy since heat treatment cannot be used to reduce the grain size once an ingot is made. The grain size can be decreased only by working either by rolling or forging. Proper attention and selection of welding parameters can improve the shape of the weld nugget, although this may not be a sufficient remedy by itself. In gas tungsten-arc welding a slow travel speed will give a favorable weld shape.

Another method which can be used is to place a strip over the joint to be welded such that all of the cracks are located in the strip which can be machined off. This does not eliminate the cracking in the alloy, but the finished joint will be free of cracks.

### Conclusions

The results of this investigation suggest the following conclusions:

1. The shape of the weld nugget plays an important role in cracking. Where the re-entrant angle of the nugget changes rapidly the cracking susceptibility in the heat-affected zone increases. The high voltage electron beam welding process tends to produce a wedge shape weld nugget with less change in re-entrant angle. The heat-affected zone of welds made by the high voltage electron beam process are less crack sensitive than those made by the low voltage process. In these tests gas tungsten-arc welds made without undercutting exhibited no microcracking in the heat-affected zone while those with undercutting did crack.

2. The cracking sensitivity of alloy 718 increases as the grain size of the base metal increases. Manganese and silicon increase the crack sensitivity when either is present in amounts greater than 0.15% by weight. The microprobe tests indicate that the grain boundaries associated with cracking are rich in columbium, carbon, titanium and molybdenum while being depleted in chromium, iron and nickel.

Finally, a mechanism of heat-affected zone cracking has been developed which suggests the cracking is caused by the combined factors of weld shape, grain size, incipient melting, stress pattern, and a weak phase in the grain boundaries.

### Acknowledgements

The authors wish to thank the Union Carbide Corporation and its Linde and Materials Systems Divisions for the fellowship program and technical assistance. Welding materials and cooperation of the International Nickel Company, Inc., Huntington Alloy Products Division are also appreciated.

### Bibliography

1. Whittle, F., "The Early History of

the Whittle Jet Propulsion Gas Turbine," Proceedings Institute Mechanical Engineers, pages 419-435 (1946).

2. Thompson, E. G., "Hot Cracking Studies of Alloy 718 Weld Heat-Affected Zones," WELDING JOURNAL, 48(2), Research Suppl., 70-s to 79-s (1969).

3. Morrison, T. J., Shira, C. S., and Weisenburg L. A., "The Influence of Minor Elements on Alloy 718 Weld Microfissuring," Welding Research Council Symposium, Houston, Texas, October, 1967.

4. Prager, M., and Shira, C. S., "Welding of Precipitation Hardening Nickel Base Alloys," Welding Research Council Bulletin 128, Feb. 1968.

5. Hudec, R. P., "Measurement of Residual Stress in a Variable Restraint Weld Specimen by X-Ray Diffraction," Ohio State University Thesis (1965).

6. Hicken, G. K., and Jackson, C. E., "The Effects of Applied Magnetic Fields on Welding Arcs," WELDING JOURNAL, 44 (11), Research Suppl., 515-s to 524-s (1966).

7. Eiselstein, H. L., "Metallurgy of a Columbium-Hardened Nickel-Chromium Iron Alloy," ASTM Meeting (June 1963).

8. Zener, C., "Elasticity and Anelasticity of Metals," The University of Chicago Press, Chicago, Illinois, 1948.

9. Personal Correspondence with General Electric Co., Evandale, Ohio.

# Technical Note: Application of SWAT to the Nondestructive Inspection of Welds

BY C. E. HARTBOWER

SWAT is an acronym for Stress Wave Analysis Technique. Stress waves are produced by the release of elastic energy resulting from the growth of a crack in a stress field. Thus, SWAT constitutes a unique nondestructive inspection method in that the material defect, when propagating, transmits its own signal, with the sensor acting as the receiver. In other words, the material undergoing crack growth both generates and transmits the signal. The SWAT system, consisting of sensors, amplifiers and filters (to eliminate extraneous low-frequency noise) serves as the receiver. System sensitivity can be preset to trigger on a selected signal amplitude, and the operational and reliability status of the system can be checked by periodically inserting a calibration signal. The util-

ity of SWAT as a new, highly sensitive method for monitoring crack growth has been demonstrated in several researches.<sup>1-7</sup>

The objective of the experiment described here was to demonstrate the feasibility of SWAT as a method for obtaining data on delayed weld cracking. In the fabrication of HY-80 submarine hulls, a minimum period of seven days is allowed before nondestructive inspection to be certain that any delayed cracking that might occur will have been completed. Obviously, if a quantitative measurement can be made of the time involved in the delayed cracking process, it may be possible to shorten the minimum time between completing a weld and nondestructive inspection and, thereby, save submarine production time.

### The Test Weldment

HY-80 steel (MIL-S-16216-G) in the form of 2-in.-wide by 10 in. long by 0.70 in. thick bars were welded to

form a test plate 8 in. wide by 10 in. long. Thus, there were three longitudinal welds 10 in. long joining four 2 in. wide bars. The joint design was simply a square butt; incomplete penetration was deliberate to assure cracking. The welding was done by the tungsten-arc process using a 600 amp, automatic welding unit and Linde-83, 1/16 in. diameter filler metal conforming to AWS-ASTM classification E-70S-G.

The welding sequence is shown in Fig. 1; note that two weldments 4 in. wide by 10 in. long were prepared first, and then joined to make the 8 in. wide x 10 in. long test weldment. Passes 1-4 and 9-10 were fusion passes (without filler metal); passes 5-13 involved filler metal automatically fed into the arc at 20 kw. The arc travel speed was 6 ipm at 350 amp and 10 v. The interpass temperature was not controlled; however, the time between passes was recorded, indicating the interpass temperature to be between 300 and 500° F. Contact-pyrometer readings taken after the final pass showed the weldment to be about 225° F at the time the SWAT system was activated.

### The SWAT System

The weldment was placed in a sound-insulated chamber at 4:30  
(Continued on page 60-s)

C. E. HARTBOWER is Associate Scientist, Materials Integrity Section, Materials Technology Dept., Solid Rocket Division, Aerojet-General Corp., Sacramento, Calif.

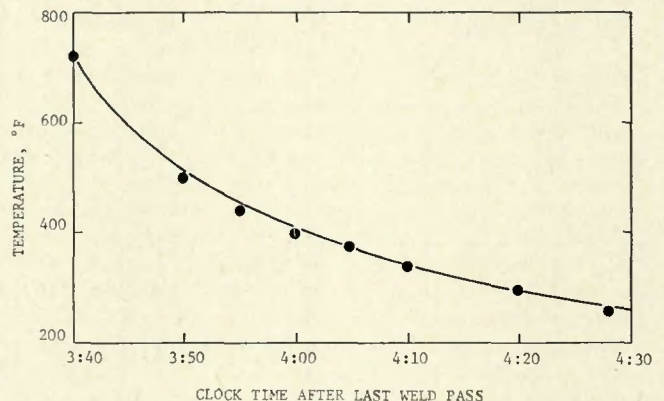
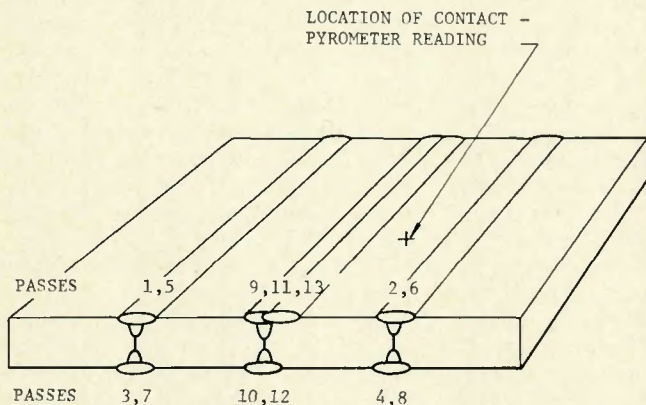


Fig. 1—Weld sequence and temperature